Needleless Electrospinning. I. A Comparison of Cylinder and Disk Nozzles

Haitao Niu, Tong Lin, Xungai Wang

Centre for Material and Fibre Innovation, Deakin University, Geelong, Victoria 3217, Australia

Received 2 November 2008; accepted 3 June 2009
DOI 10.1002/app.30891
Published online 12 August 2009 in Wiley InterScience (www.interscience.wiley.com).

ABSTRACT: In this study, we demonstrated the needleless electrospinning of poly(vinyl alcohol) (PVA) nanofibers with two nozzles, a rotating disk and a cylinder, and examined the effect of the nozzle shape on the electrospinning process and resultant fiber morphology. The disk nozzle needed a relatively low applied voltage to initiate fiber formation, and the fibers were mainly formed on the top disk edge. Also, the PVA concentration had little influence on the disk electrospinning process (up to 11 wt %). In comparison, the cylinder electrospinning showed a higher dependence on the applied voltage and polymer concentration. The fibers were initiated from the cylinder ends first and then from the entire cylinder surface only if the applied voltage were increased to a certain level. With the same polymer solution, the critical voltage needed to generate nanofibers from the disk nozzle was lower than that needed to generate nanofibers from the cylinder. Both electrospinning systems could produce uniform nanofibers, but the fibers produced from the disk nozzle were finer than those from the cylinder when the operating conditions were the same. A thin disk (8 cm in diameter and 2 mm thick) could produce nanofibers at a rate similar to that of a cylinder of the same diameter but 100 times wider (i.e., 20 cm long). Finite element analysis of electric field profiles of the nozzles revealed a concentrated electric field on the disk edge. For the cylinder nozzle, an uneven distribution of the electric field intensity profile along the nozzle surface was observed. The field lines were mainly concentrated on the cylinder ends, with a much lower electric field intensity formed in the middle surface area. At the same applied voltage, the electric field intensity on the disk edge was much higher than that on the cylinder end. These differences in the electric field intensity profiles could explain the differences in the fiber fineness and rate of the nanofibers produced from these two nozzles. These findings will benefit the design and further development of large-scale electrospinning systems for the mass production of nanofibers for advanced applications. © 2009 Wiley Periodicals, Inc. J Appl Polym Sci 114: 3524–3530, 2009

Key words: extrusion; fibers; nanotechnology

INTRODUCTION

As a simple and efficient nanofiber-making technique, electrospinning has substantial adaptability for processing a variety of polymers with possible control of the fiber fineness,[1–4] orientation,[5] surface morphology,[6] and bicomponent cross-sectional configuration.[7,8] Electrospun nanofibers have enormous application potential in areas as diverse as tissue engineering scaffolds,[9,10] wound healing,[11] release control,[12–14] filtration,[15,16] reinforcement,[17] protective clothing,[18,19] sensors,[20,21] catalysis,[22] and energy conversion and storage.[23]

A conventional electrospinning setup typically comprises a high-voltage power supply, a collector, and a spinneret (or nozzle).[24] A hollow needle (e.g., a syringe needle or glass Pasteur pipette) is normally used as a nozzle to produce polymer jets/filaments. Because each needle can produce only one polymer jet, needle electrospinning systems have very low productivity (<300 mg/h per needle). How to electrospin nanofibers on a large scale has been an issue of concern, and further development is warranted to facilitate the commercial application of nanofibers.

The main strategy for improving electrospinning production has been based on increasing the number of needle nozzles.[25,26] However, a multineedle spinneret needs a large operating space and careful design of the relative spacing between the needles so that strong charge repulsion between the jets and adjacent needles and associated uneven fiber deposition can be avoided. In addition, using a gas jacket has been reported to enhance the processability of a single-needle nozzle.[27,28] The gas jacket, however, influences the nanofiber morphology and fineness.

Recently, needleless electrospinning setups have been developed. Without a needle nozzle, a number of jets can be generated even from a widely open liquid surface. The pioneering work was reported by Yarin and Zussman,[29] who used a magnetic fluid to

Correspondence to: T. Lin (tong.lin@deakin.edu.au).

Contract grant sponsor: Australian Research Council; contract grant number: ARC LP0776751.

Contract grant sponsor: Deakin University Central Research Grant scheme.

Journal of Applied Polymer Science, Vol. 114, 3524–3530 (2009)

agitate the uppermost polymer solution to initiate the concurrent production of multiple jets from a flat polymer solution surface. Later, Jirsak et al.[30] described the generation of multiple jets from a liquid uploaded on a slowly rotating horizontal cylinder, which was subsequently commercialized by Elmarco under the brand name Nanospider. In addition, Dosunmu et al.[31] reported the formation of multiple jets using a tubular plastic foam spinneret.

The generation of multiple jets from a needleless spinneret has been explained as follows: the waves of an electrically conductive liquid self-organize on a mesoscopic scale and finally form jets when the applied electric field intensity is above a critical value.[32] Therefore, the jet initiation and resulting fiber morphology are highly influenced by the electric field intensity profile around the spinneret and in the electrospinning zone, which is governed by the applied voltage and the shape of the needleless spinneret. Nevertheless, little has been reported in the literature on how the applied voltage and nozzle structure influence the needleless electrospinning process and resulting fiber morphology.

In this article, we report the electrospinning of poly(vinyl alcohol) (PVA) with two different needleless nozzles, a cylinder and a disk. In comparing the electrospinning process and as-spun fiber morphology, we have found that the disk nozzle requires a lower applied voltage in electrospinning to initiate jets/filaments than the cylinder nozzle, and the fibers electrospun from the disk nozzle are finer than those from the cylinder nozzle. These differences are discussed in terms of differences in the electric field intensity profile between the two electrospinning systems.

EXPERIMENTAL

Materials and measurement

PVA (weight-average molecular weight = 146,000–186,000, 98–99% hydrolyzed) was obtained from Aldrich (USA) and used as received. A PVA solution was prepared by the dissolution of PVA in distilled water followed by vigorous stirring for 6 h at 85°C. The PVA concentration was in the range of 8.0–11.0 wt %.

The fiber morphologies were observed by scanning electron microscopy (SEM; S440, Leica, Cambridge, England), and the average fiber diameters were calculated on the basis of the SEM images with image analysis software (ImagePro Plus 4.5). The electric fields were calculated by the finite element method with the program FEMLAB3.4.

Electrospinning

Figure 1 illustrates the needleless electrospinning setups, which contained a rotary aluminum spinneret (disk or cylinder), a Teflon solution vessel, a high-voltage direct-current power supply (ES50P-20 W/DAM, Gamma High Voltage Research, USA), and a grounded drum collector. The cylinder nozzle was 20 cm long and 8 cm in diameter, whereas the disk nozzle had the same diameter as the cylinder, but the thickness was 2 mm. The edges of both the cylinder and disk were beveled, and the radius of the beveled curve was about 5 mm.

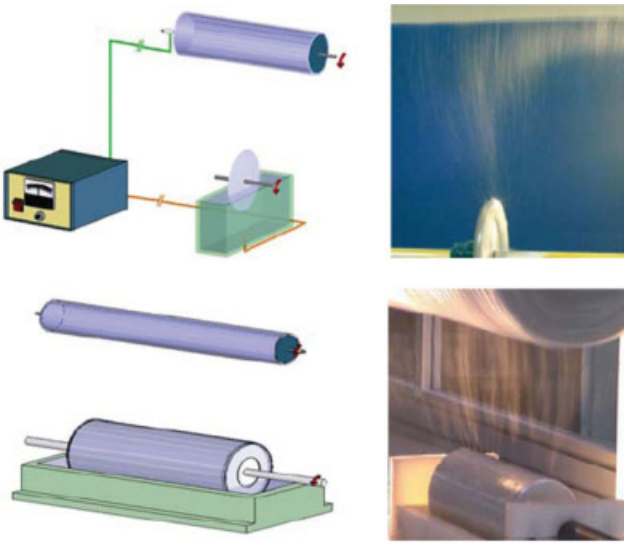

Figure 1 Apparatuses for disk and cylinder electrospinning and photos of the two electrospinning processes. [Color figure can be viewed in the online issue, which is available at www.interscience.wiley.com.]

During electrospinning, the vessel was filled with the PVA solution so that nearly half of the spinneret was immersed in the polymer solution, and the unimmersed part of the spinneret was covered with a thin layer of the PVA solution via rotation. When the PVA solution was charged with a high electrical voltage via a copper wire inside the solution vessel, numerous jets/filaments were generated from the spinneret, which were deposited on the rotating drum collector. With the rotation of the spinneret, the PVA solution was loaded onto the spinneret surface constantly, and this led to the continuous generation of polymer jets/filaments.

RESULTS AND DISCUSSION

The electrospinning processes for both the cylinder and disk electrospinning systems are also demonstrated in Figure 1. During electrospinning, a number of jets were observed to be generated simultaneously from both nozzles, and the formation of jets/filaments was influenced by the spinneret rotating speed, the applied voltage, and the polymer concentration.

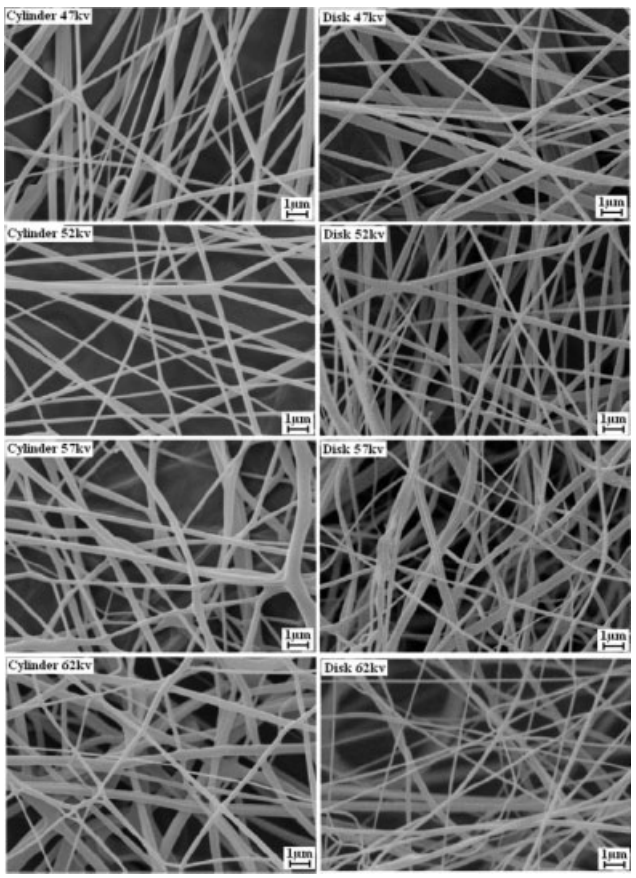

Figure 2 SEM images of the PVA nanofibers electrospun by disk and cylinder nozzles under different applied voltages (PVA concentration = 9.0 wt %, spinning distance = 13 cm). (At 47 and 52 kV, the fibers were generated only from the cylinder ends).

The spinneret rotating speed affected the loading of the PVA solution on the nozzle surface. When the rotating speed was less than 20 rpm, uneven solution coverage became apparent, and jets could not be generated continuously. Higher rotating speeds, in the range of 40–50 rpm, enabled the nozzle surface to be covered evenly with a thin layer of the PVA solution, and jets/filaments were thus generated in a continuous way. However, further increasing the rotating speed could throw the polymer solution off the spinneret.

The applied voltage is a very important parameter affecting the formation of jets/filaments. For the disk nozzle, no jet was formed when the applied voltage was lower than 42 kV. When the applied voltage was higher than such a critical voltage, the jets were generated mainly on the edge side of the disk, about 5 mm in width. Increasing the applied voltage showed little influence on the electrospinning process until the voltage reached 62 kV, above which the working current in the power supply was too high to allow normal operation of the power supply.

In comparison, electrospinning using the cylinder nozzle showed a higher dependence on the applied voltage. The critical applied voltage for generating jets from the cylinder nozzle was about 47 kV. Despite the high applied voltage, the jets were just generated from two end areas (ca. 2 cm wide) on the cylinder surface. A few jets were also observed to be produced on two sides of the cylinder. There was no jet/filament produced from the middle cylinder surface until the applied voltage was above 57 kV. Further increasing the applied voltage led to the generation of jets from the entire cylinder surface, as illustrated in Figure 1.

Besides the electrospinning process, the fiber morphology was also influenced by the applied voltage. The SEM images of nanofibers electrospun by both the cylinder and disk systems from 9.0 wt % PVA solutions under different applied voltages are shown in Figure 2. The average fiber diameters calculated on the basis of the SEM images are given in Figure 3(a).

Nanofibers electrospun from the disk nozzle showed a bead-free fibrous structure. With an increase in the applied voltage from 47 to 62 kV, the average fiber diameter was reduced from 340 to 194 nm, and the diameter distribution became narrower also. For the cylinder nozzle, the average fiber

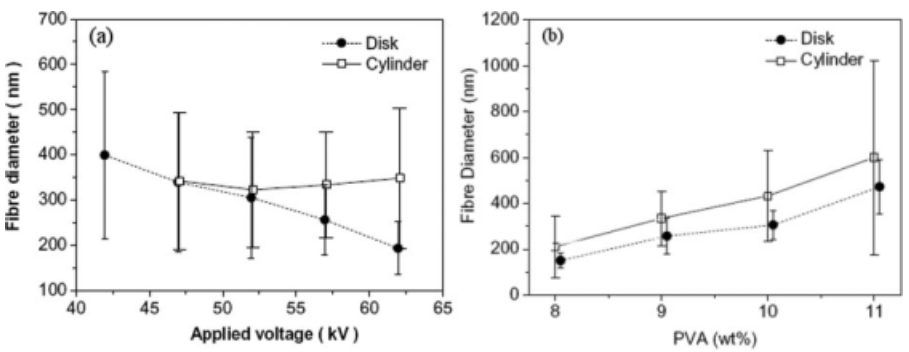

Figure 3 Dependence of the average fiber diameter on the (a) applied voltage (PVA = 9 wt %, collecting distance = 13 cm) and (b) PVA concentration (collecting distance = 13 cm, applied voltage = 57 kV).

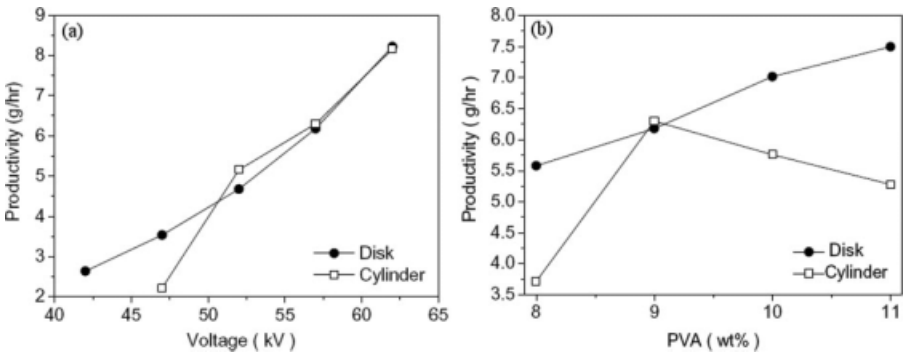

Figure 4 Productivity of the nanofibers under different (a) applied voltages (PVA = 9 wt %) and (b) PVA concentrations (applied voltage = 57 kV).

diameter and diameter distribution showed a very small dependence on the applied voltage. The variation of the applied voltage between 47 and 62 kV led to little change in the fiber diameter and distribution, although the fibers were produced at the cylinder ends only when the applied was lower than 57 kV. At the same applied voltage, the nanofibers electrospun from the disk nozzle were slightly finer than those from the cylinder nozzle, and the higher the applied voltage was, the finer the fibers were that were produced by the disk nozzle.

The distance between the spinneret and collector also influenced the electrospinning process and fiber morphology. It was noticed that the distance between the nozzle and collector for the disk electrospinning system could be adjusted between 11 and 19 cm. A shorter spinning distance led to wet fibers that merged into a polymer film on the collector, whereas a longer spinning distance resulted in stoppage of electrospinning because of a weak electric field. For the cylinder electrospinning system, the range of electrospinning distances was narrower (11–15 cm).

The polymer concentration was an important factor affecting the electrospinning process and fiber morphology.[33] With the applied voltage of 57 kV, the nanofibers electrospun from both systems showed an increased fiber diameter with the increase in the PVA concentration. The as-spun fibers from the disk nozzle had finer fibers with a much narrower diameter distribution than those from the cylinder nozzle [Fig. 3(b)].

The electrospinning process with the cylinder nozzle was highly influenced by the polymer concentration. When the PVA concentration was below 9.0 wt %, nanofibers were electrospun from the whole cylinder surface if the applied voltage was greater than 52 kV. When the PVA concentration was larger than 9.0%, the higher solution viscosity (>1620 cP) resulted in stoppage of electrospinning from the middle cylinder surface, although the nanofibers were still spun by the cylinder ends. However, nanofibers could still be generated from the middle cylinder surface if a higher applied voltage was employed. Also, a higher PVA concentration led to a reduction in the fiber-generating zone at the cylinder ends. In comparison, the nanofibers electrospun from the disk nozzle showed a lower dependence on the PVA concentration. When the PVA concentration was in the range of 8.0–11.0 wt %, the solution could always be electrospun by the disk nozzle.

The productivity of cylinder electrospinning was influenced by the applied voltage and polymer concentration. As shown in Figure 4, with the increase in the applied voltage, the production rate increased for both electrospinning systems. At a high applied voltage, the productivities of the two electrospinning systems were very similar, although the cylinder nozzle was 100 times longer (wider) than the disk nozzle. Under the same applied voltage (57 kV), with the increase in the polymer concentration, the productivity of disk electrospinning increased constantly, whereas for the cylinder electrospinning system, the productivity increased initially but decreased when the PVA concentration was greater than 9 wt %. The reason for the reduced productivity at the increased PVA concentration was the high solution viscosity, which restricted jet/filament formation.

To understand these experimental results, the electric field profiles around the nozzle surface and in the electrospinning zone (from the tip of the spinneret to the collector) were calculated by finite element analysis. As shown in Figure 5(a,b), the disk nozzle possessed a different electric field profile than the cylinder nozzle. The field lines around the disk nozzle were concentrated on the top peripheral edge area. However, the electric field on the cylinder was concentrated on the cylinder ends.

The electric field intensity along the cylinder surface is shown in Figure 6(a). A high electric field intensity was formed at the cylinder end areas, and the intensity decreased gradually toward the middle surface. Because the jet initiation was highly

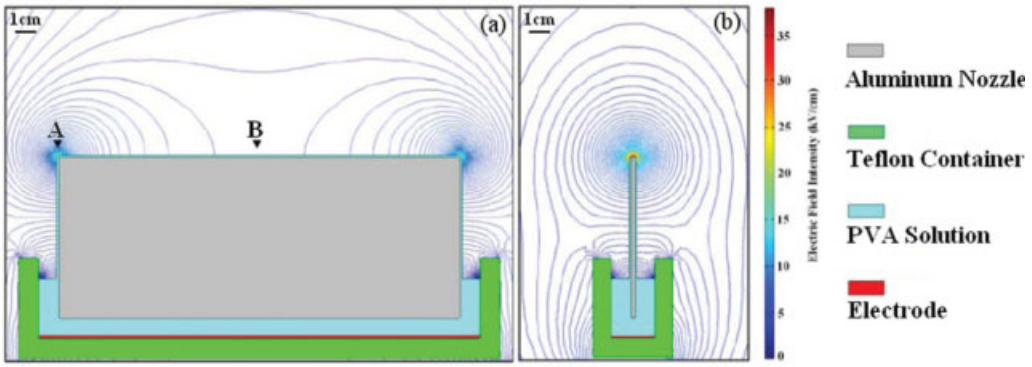

Figure 5 Electric field profile around the (a) cylinder nozzle and (b) disk nozzle. [Color figure can be viewed in the online issue, which is available at www.interscience.wiley.com.]

determined by the electric field intensity around the nozzle surface, the areas with higher electric field intensity generated nanofibers more easily. The higher electric field intensity at the cylinder ends versus the middle cylinder surface could be the main reason that the jets/filaments were generated only from the ends of the cylinder surface when the applied voltage was low. For the disk nozzle, the highest electric field intensity was on the top edge of the disk, and the electric field intensity decayed from the top disk edge toward the liquid surface [Fig. 6(b)]. With the increase in the applied voltage, the electric field intensity increased on the surface.

On the basis of the experimental finding that the jets started to generate on the disk edge when the applied voltage was higher than 42 kV, the lowest surface electric field intensity that could initiate the formation of jets on the disk nozzle could be

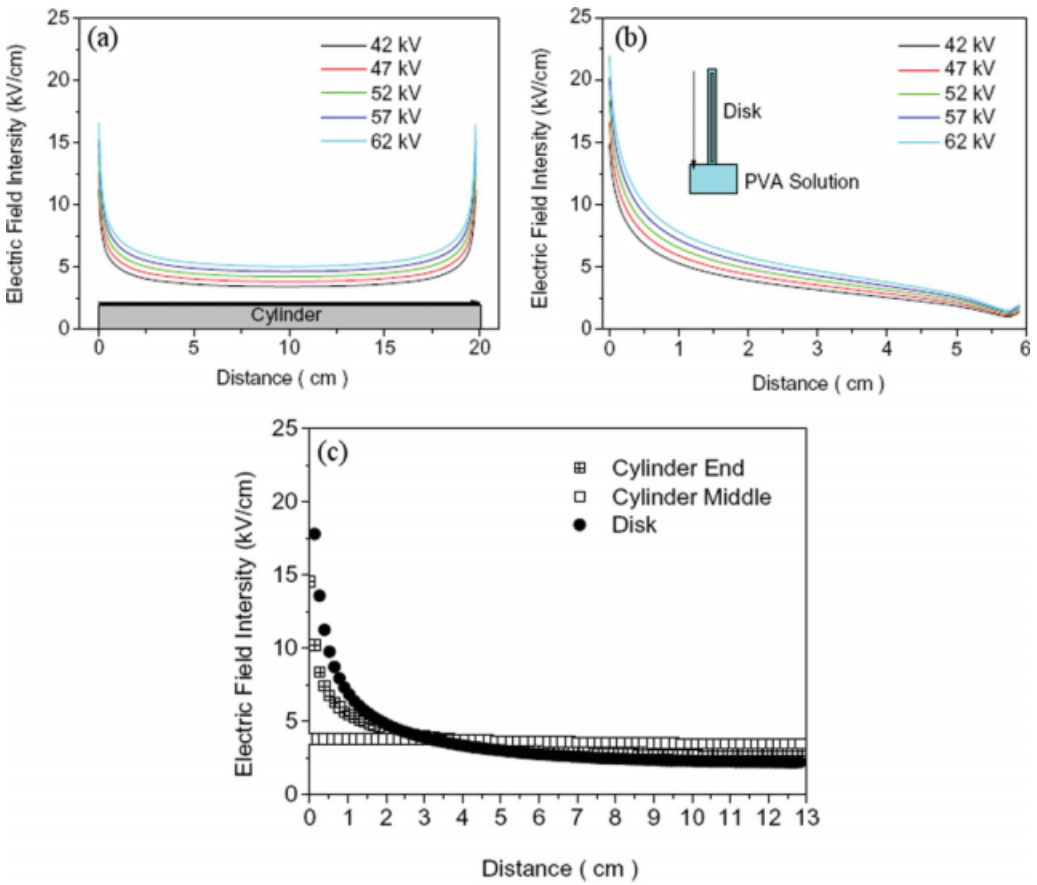

Figure 6 Electric field intensity along the (a) surface of the cylinder, (b) surface of the disk under different applied voltages, and (c) electrospinning direction [nozzle (0,0), collector (0,13), applied voltage = 57 kV]. [Color figure can be viewed in the online issue, which is available at www.interscience.wiley.com.]

calculated to be 5 kV/cm. A similar value could also be obtained from the cylinder nozzle on both end and middle surfaces. Therefore, 5 kV/cm could be the critical electric field intensity at which the surface could electrospin nanofibers with a 9.0 wt % PVA solution.

Figure 6(c) shows the electric field intensity profile from the nozzle surface to the collector. For the disk system, the electric field near the tip of the disk decayed rapidly in the first few centimeters away from the spinneret and stabilized toward the collector. For the cylinder nozzle, only the cylinder ends showed an electric field profile similar to that of the disk nozzle, but the electric field intensity was lower than that at the disk edge. The electric field intensity at the middle cylinder surface was far lower than that at the cylinder ends, and the electric field intensity decayed slowly toward the collector.

As the electric field is the main driving force to initiate the formation of a polymer jet,[34] a polymer solution charged by an electric field of a higher intensity can more easily generate jets, and the jets should be stretched under stronger forces, thus producing finer fibers. The uneven distribution of the electric field intensity along the cylinder nozzle surface leads to coarser nanofibers generated from the middle cylinder surface in comparison with those produced from the cylinder ends. As a result of fibers being collected from the entire cylinder nozzle, the nanofibers have a wide diameter distribution, and the average fiber diameter is less affected by the applied voltage. In comparison, the distribution of the electric field intensity on the top disk edges is sharper and narrower, resembling that at the cylinder ends, albeit higher in intensity; this leads to finer fibers with a narrower diameter distribution, and the average diameter shows an apparent dependence on the applied voltage.

The electric field also functions to overcome the frictional forces that act within the moving polymer solution and to accelerate filament movement toward the collector electrode. This is why a higher electric field can cause higher mass flow to be electrospun and hence greater fiber productivity.[35,36] In the case of electrospinning with a rotating nozzle, in which a thin layer of the polymer solution is electrospun, the rapid removal of the polymer solution from the limited volume of the polymer solution in the fiber-generating zone results in a thinner solution layer on the nozzle surface. The additional resistance from the solid–liquid boundary layer effect becomes an important factor retaining the surface solution.

If the electric field is strong enough, the mass flow will be controlled mainly by the fluid thickness and the boundary layer resistance induced by the mass transfer. Under the same operating conditions, a more viscous solution tends to form a thicker solution layer on the nozzle surface. The increased solution volume in the fiber-generating area helps to reduce the boundary layer resistance, resulting in higher mass flow. On the contrary, the higher solution viscosity also leads to a reduction in mass flow. The two opposite trends could make the mass flow remain unchanged, and this can be demonstrated by disk electrospinning. Although the fiber productivity for disk electrospinning increased with the PVA concentration, the mass flows, calculated on the basis of the production rate, were quite similar, in the range of 68–70 mL/h, for the three polymer solutions (9.0, 10.0, and 11.0%).

In comparison, if the electric field is just above the critical value needed to initiate jet formation, the low mass flow will leave a thicker solution layer on the nozzle surface. In this case, the boundary layer resistance is weaker, and the solution viscosity dominates the mass flow. Increasing the solution viscosity will decrease the jet number, and this will result in lower mass flow and productivity. This should be the main reason that the fiber productivity for cylinder electrospinning decreases with an increase in the polymer concentration.

CONCLUSIONS

In this work, we have demonstrated that PVA nanofibers can be electrospun from the surfaces of a rotating metal disk and a cylinder. For the disk electrospinning, nanofibers were mainly produced from the disk edge area, and the voltage for initiating the electrospinning process was 42 kV (9.0 wt % PVA). With the increase in the applied voltage, the disk-spun nanofibers became finer with a narrower diameter distribution. In comparison, nanofibers from the cylinder nozzle were mainly produced from the cylinder surface, but the area in which the nanofibers were generated was highly dependent on the applied voltage and the polymer concentration. When the applied voltage was above a critical value, nanofibers started to be generated at the cylinder end areas. Only at a higher applied voltage could the nanofibers be generated from the entire cylinder surface. With increased polymer concentration, a higher critical voltage was necessary to initiate nanofibers from the cylinder surface because of increased solution viscosity. For the same polymer solution (9.0 wt % PVA), the critical voltage for the generation of polymer jets from the cylinder end was 47 kV, and the critical voltage for producing polymer jets from the entire cylinder surface was 57 kV. When the applied voltage was increased, nanofibers produced by the cylinder nozzle showed a similar fineness and diameter distribution. Under the same operating conditions, nanofibers generated from the disk nozzles

were finer with a narrower distribution than those produced by the cylinder.

The fiber productivity increased with the applied voltage for both electrospinning systems. Although the disk nozzle took much less space than the cylinder nozzle of the same diameter, the production rates of the two needleless electrospinning systems were similar.

By analyzing the electric field around the nozzles and in the electrospinning zone, we observed that the disk electrospinning had a much different electric field profile than the cylinder one. For the disk nozzle, the field lines were mainly concentrated on the disk edge, whereas the cylinder nozzle showed concentrated field lines at the cylinder ends. The different electric field concentration could be the reason for the uneven generation of nanofibers on the nozzle surface. By combining the calculation with the experimental observation, we obtained the critical value of the surface electric field intensity for generating nanofibers: 5 kV/cm. This critical value provides a very useful guide for the design of new needleless electrospinning systems. Although the results presented in this article were focused on PVA polymer, our recent work has confirmed that other water-soluble polymers [e.g., poly(vinyl pyrrolidone)] can also be electrospun in a similar way.

References

1. Reneker, D. H.; Chun, I. Nanotechnology 1996, 7, 216.
2. Jayaraman, K.; Kotaki, M.; Zhang, Y.; Mo, X.; Ramakrishna, S. J Nanosci Nanotechnol 2004, 4, 52.
3. Li, D.; Xia, Y. Adv Mater 2004, 16, 1151.
4. Greiner, A.; Wendorff, J. H. Angew Chem Int Ed 2007, 46, 5670.
5. Li, D.; Wang, Y.; Xia, Y. Nano Lett 2003, 3, 1167.
6. Casper, C. L.; Stephens, J. S.; Tassi, N. G.; Chase, D. B.; Rabolt, J. F. Macromolecules 2004, 37, 573.
7. Sun, Z.; Zussman, E.; Yarin, A. L.; Wendorff, J. H.; Greiner, A. Adv Mater 2003, 15, 1929.
8. Lin, T.; Wang, H.; Wang, X. Adv Mater 2005, 17, 2699.
9. Matthews, J. A.; Wnek, G. E.; Simpson, D. G.; Bowlin, G. L. Biomacromolecules 2002, 3, 232.
10. Kenawy, E.-R.; Layman, J. M.; Watkins, J. R.; Bowlin, G. L.; Matthews, J. A.; Simpson, D. G.; Wnek, G. E. Biomaterials 2003, 24, 907.
11. Khil, M. S.; Cha, D. I.; Kim, H. Y.; Kim, I. S.; Bhattarai, N. J Biomed Mater Res B 2003, 67, 675.
12. Kenawy, E. R.; Bowlin, G. L.; Mansfield, K.; Layman, J.; Simpson, D. G.; Sanders, E. H.; Wnek, G. E. J Controlled Release 2002, 81, 57.
13. Kim, K.; Luu, Y. K.; Chang, C.; Fang, D.; Hsiao, B. S.; Chu, B.; Hadjiargyrou, M. J Controlled Release 2004, 98, 47.
14. Luong-Van, E.; Grrndahl, L.; Chua, K. N.; Leong, K. W.; Nurcombe, V.; Cool, S. M. Biomaterials 2006, 27, 2042.
15. Suthar, A.; Chase, G. TCE 2001, 726, 26.
16. Suthar, A.; Chase, G. Adv Filtr Sep Technol 2002, 15, 265.
17. Bergshoef, M. M.; Vancso, G. J. Adv Mater 1999, 11, 1362.
18. Gibson, P.; Schreuder-Gibson, H. MD (American Society of Mechanical Engineers), 2000, 91, 45.
19. Gibson, P.; Schreuder-Gibson, H.; Rivin, D. Colloid Surf A 2001, 187–188, 469.
20. Wang, X.; Drew, C.; Lee, S. H.; Senecal, K. J.; Kumar, J.; Samuelson, L. A. Nano Lett 2002, 2, 1273.
21. Wang, X.; Kim, Y.-G.; Drew, C.; Ku, B.-C.; Kumar, J.; Samuelson, L. A. Nano Lett 2004, 4, 331.
22. Demir, M. M.; Gulgun, M. A.; Menceloglu, Y. Z.; Erman, B.; Abramchuk, S. S.; Makhaeva, E. E.; Khokhlov, A. R.; Matveeva, V. G.; Sulman, M. G. Macromolecules 2004, 37, 1787.
23. Choi, S. W.; Jo, S. M.; Lee, W. S.; Kim, Y.-R. Adv Mater 2003, 15, 2027.
24. Megelski, S.; Chase, J. S. S. D. B.; Rabolt, J. F. Macromolecules 2002, 35, 8456.
25. Ding, B.; Kimura, E.; Sato, T.; Fujita, S.; Shiratori, S. Polymer 2004, 45, 1895.
26. Theron, S. A.; Yarin, A. L.; Zussman, E.; Kroll, E. Polymer 2005, 46, 2889.
27. Um, I. C.; Fang, D.; Hsiao, B. S.; Okamoto, A.; Chu, B. Biomacromolecules 2004, 5, 1428.
28. Larsen, G.; Spretz, R.; Velarde-Ortiz, R. Adv Mater 2004, 16, 166.
29. Yarin, A. L.; Zussman, E. Polymer 2004, 45, 2977.
30. Jirsak, O.; Sanetrnik, F.; Lukas, D.; Kotek, V.; Martinova, L.; Chaluopek, J. International Pat., WO 2005/024101 (2005).
31. Dosunmu, O. O.; Chase, G. G.; Kataphinan, W.; Reneker, D. H. Nanotechnology 2006, 17, 1123.
32. Lukas, D.; Sarkar, A.; Pokorny, P. J Appl Phys 2008, 103, 084309/1.
33. Eda, G.; Shivkumar, S. J Appl Polym Sci 2007, 106, 475.
34. Deitzel, J. M.; Kleinmeyer, J.; Harris, D.; Tan, N. C. B. Polymer 2001, 42, 8163.
35. Demira, M. M.; Yilgorb, I.; Yilgorb, E.; Erman, B. Polymer 2002, 43, 3303.
36. Wang, X.; Niu, H.; Lin, T.; Wang, X. Polym Eng Sci 2009, 49, 1582.